AJNR

Subcortical Ischemic Vascular Dementia: Assessment with Quantitative MR Imaging and 1 H MR Spectroscopy

Aristides A. Capizzano, Norbert Schuff, Diane L. Amend, Jody L. Tanabe, David Norman, Andrew A. Maudsley, William Jagust, Helena C. Chui, George Fein, Mark R. Segal and Michael W. Weiner

AJNR Am J Neuroradiol 2000, 21 (4) 621-630
http://www.ajnr.org/content/21/4/621

AJNR Am J Neuroradiol 21:621–630, April 2000

Subcortical Ischemic Vascular Dementia: Assessment with Quantitative MR Imaging and ^{1}H MR Spectroscopy

Aristides A. Capizzano, Norbert Schuff, Diane L. Amend, Jody L. Tanabe, David Norman, Andrew A. Maudsley, William Jagust, Helena C. Chui, George Fein, Mark R. Segal, and Michael W. Weiner

BACKGROUND AND PURPOSE: **Subcortical ischemic vascular dementia is associated with cortical hypometabolism and hypoperfusion, and this reduced cortical metabolism or blood flow can be detected with functional imaging such as positron emission tomography. The aim of this study was to characterize, by means of MR imaging and ^{1}H MR spectroscopy, the structural and metabolic brain changes that occur among patients with subcortical ischemic vascular dementia compared with those of elderly control volunteers and patients with Alzheimer's disease.**

METHODS: **Patients with dementia and lacunes (n = 11), cognitive impairment and lacunes (n = 14), and dementia without lacunes (n = 18) and healthy age-matched control volunteers (n = 20) underwent MR imaging and ^{1}H MR spectroscopy. ^{1}H MR spectroscopy data were coanalyzed with coregistered segmented MR images to account for atrophy and tissue composition.**

RESULTS: **Compared with healthy control volunteers, patients with dementia and lacunes had 11.74% lower *N*-acetylaspartate/creatine ratios (NAA/Cr) ($P = .007$) and 10.25% lower *N*-acetylaspartate measurements (NAA) in the cerebral cortex ($P = .03$). In white matter, patients with dementia and lacunes showed a 10.56% NAA/Cr reduction ($P = .01$) and a 12.64% NAA reduction ($P = .04$) compared with control subjects. NAA in the frontal cortex was negatively correlated with the volume of white matter signal hyperintensity among patients with cognitive impairment and lacunes ($P = .002$). Patients with dementia, but not patients with dementia and lacunes, showed a 10.33% NAA/Cr decrease ($P = .02$) in the hippocampus compared with healthy control volunteers.**

CONCLUSION: **Patients with dementia and lacunes have reduced NAA and NAA/Cr in both cortical and white matter regions. Cortical changes may result from cortical ischemia/infarction, retrograde or trans-synaptic injury (or both) secondary to subcortical neuronal loss, or concurrent Alzheimer's pathologic abnormalities. Cortical derangement may contribute to dementia among patients with subcortical infarction.**

Vascular dementia is the second most common type of dementia in the elderly after Alzheimer's disease (1–4). Vascular dementia comprises different entities that result in cognitive decline from vascular cause (5). In addition to multi-infarct dementia, small-vessel disease is highly prevalent (6). The latter is associated with subcortical lesions such as lacunes (7) and incomplete white matter types of infarction (8–10). Considering the diversity of vascular dementia, studies of this entity need to recognize its subtypes. We limited our study to subcortical ischemic vascular dementia, excluding patients with cortical infarcts. Functional neuroimaging techniques such as positron emission tomography, single-photon emission CT, and stable xenon-enhanced CT reveal reduced cortical metabolism or blood flow or both in cases of subcortical ischemic vascular dementia (11–18). MR imaging reveals atrophy and white matter signal hyperintensity (19). Neuropathologic studies, however, have shown that myelinic and axonal loss might be undetectable with MR imaging (20). Furthermore, MR imaging cannot show the difference between neurons and glial cells. Because vascular dementia

Received July 6, 1999; accepted after revision November 18.

From the Department of Veterans Affairs Medical Center (A.A.C., N.S., D.L.A., J.L.T., A.A.M., M.W.W.), Magnetic Resonance Spectroscopy Unit, San Francisco, CA; the Departments of Radiology (A.A.C., N.S., D.L.A., J.L.T., D.N., M.W.W.), Medicine (M.W.W.), Psychiatry (G.F., M.W.W.), and Neurology (M.W.W.) and the Division of Biostatistics (M.R.S.), University of California, San Francisco, San Francisco, CA; The Center for Functional Imaging (W.J.), Ernest Orlando Lawrence Berkeley National Laboratory, Berkeley, CA; and the Department of Neurology (H.C.C.), University of Southern California, Rancho Los Amigos Medical Center, Downey, CA.

Presented as a poster at the 7th Annual ISMRM Meeting, May 1999, Philadelphia, PA.

This work was supported by National Institutes of Health grants PO1 AG12435 and RO1 AG10897.

Address reprint requests to Michael W. Weiner, MD, Magnetic Resonance Unit (114M) Department of Veterans Affairs Medical Center, 4150 Clement Street, San Francisco, CA 94121.

TABLE 1: Subjects' categories and clinical diagnoses

Clinical Diagnosis	D (n = 18)	D + Lac (n = 11)	CI + Lac (n = 14)	HC (n = 20)
Possible AD	3	1	⋯	⋯
Probable AD	14	⋯	⋯	⋯
Probable IVD	⋯	7	⋯	⋯
Definite IVD	⋯	⋯	2	⋯
Definite mixed dementia	1	⋯	⋯	⋯
Mixed dementia	⋯	3	⋯	⋯
Cognitive impairment not demented	⋯	⋯	9	⋯
Stroke w/o cognitive impairment	⋯	⋯	2	⋯
Cognitive impairment w/o stroke	⋯	⋯	⋯	1
Amnesic syndrome	⋯	⋯	1	⋯
Healthy control subjects	⋯	⋯	⋯	19
Age (yrs)	75.6 ± 7	77.7 ± 5	72.5 ± 6.9	72.8 ± 7.2
Female/male	12/6	3/8	3/11	11/9
MMSE score	16.9 ± 7.5	20.6 ± 3.4	27.5 ± 2.2	29 ± 0.8

Note.—D = demented without lacunes, D + Lac = demented with lacunes, CI + Lac = cognitively impaired with lacunes, HC = healthy control subjects, cognitive impairment = cognitive impairment not meeting criteria for dementia. Possible and probable AD defined according to NINCDS-ADRDA criteria. Probable IVD, and mixed dementia defined according to the State of California ADDTC criteria. Age and MMSE scores are reported as mean ± SD.

and Alzheimer's disease are associated with gliosis (4, 21), one interpreting MR results may underestimate neuronal loss because tissue shrinkage is attenuated by gliosis. ^{1}H MR spectroscopy reveals the presence of the amino acid *N*-acetylaspartate (NAA), which is localized exclusively in the neuron (22), and is thus expected to be a more sensitive indicator of neuronal loss than is tissue shrinkage. Previous studies (23–32) found reduced NAA in association with vascular dementia and Alzheimer's disease in different brain regions.

The present study had several goals: 1) to extend previous studies (23–32), using a multisection MR spectroscopic technique to measure brain metabolite distribution, including the cortex; 2) to determine the spatial distribution of neuronal loss and metabolic impairment in association with dementia, as measured by NAA changes; 3) to determine whether cortical NAA levels correlate with the extent of subcortical disease as measured by the number of lacunes and the volume of white matter signal hyperintensity; 4) to examine the correlation between the degree of cognitive impairment as measured by the Mini-Mental Status Examination (MMSE) and the amount of structural or metabolic changes or both; and 5) to determine which MR measures are best correlated with the cognitive status of patients with lacunes.

Methods

Participants

A total of 63 participants were entered in this study. Table 1 shows participant demographics and the correspondence between study categories and clinical diagnoses. Participants were categorized according to the presence of at least one lacunar infarction on MR images and their Clinical Dementia Rating (CDR) scores. In this study, separation of lacunes from perivascular spaces was achieved according to the following protocol. Images with CSF-like signal features in the anterior commissure were considered perivascular spaces; features outside that location and larger than 3 mm were considered cavitated lacunes and, when smaller than 3 mm, perivascular spaces. T1-, T2-, and proton density–weighted images were used by a neuroradiologist (D.N.) to assess the presence of lacunes.

Patient classification was not based on clinical diagnoses because of the uncertainty involved (33, 34). Patients were divided into the following groups: 1) the cognitively impaired with lacunes (presence of lacune(s) and CDR score of 0.5 [CI + Lac]); 2) patients with dementia and lacunes (presence of lacune(s) and CDR score of 1 [D + Lac]); 3) patients with dementia and no lacunes (no lacunes and CDR score of 1 [D]); 4) healthy volunteers (no lacunes and CDR score of 0 [HC]). The average number of supratentorial lacunes ± SD was 3.8 ± 3 for D + Lac patients and 4.3 ± 5 for CI + Lac patients. Exclusionary criteria for all participants were history of cortical stroke or other major neurologic disorder, psychiatric disorders after the age of 50 years, substance abuse, seizures, and abnormal thyroid metabolism. All participants or their legal guardians provided informed consent, which was approved by the Committee of Human Research of the University of California, San Francisco. Clinical diagnoses were made according to the criteria set forth by the National Institute of Neurological and Communicative Disorders and Stroke-Alzheimer's Disease and Related Disorders Associations for Alzheimer's disease (35) and by the State of California Alzheimer's Disease Diagnostic and Treatment Center criteria for ischemic vascular dementia proposed by Chui et al (33).

MR Imaging and MR Spectroscopy Acquisition

All MR data were acquired on a 1.5-T Magnetom VISION system (Siemens, Erlangen, Germany) equipped with a standard circularly polarized head coil. The following image sequences were acquired: 1) oblique axial T1-weighted parallel to the long axis of the hippocampus (240/14 [TR/TE]; flip angle, 60°; section thickness, 3 mm); 2) oblique axial proton density–weighted and T2-weighted double spin-echo oriented along the optic nerves (2550/20, 80; in-plane resolution, 1.4 × 1 mm^2; section thickness, 3 mm); and 3) coronal 3D T1-weighted gradient-echo orthogonal to the optic nerves (MPRAGE: 10/4; flip angle, 15°; in-plane resolution, 1.0 × 1.0 mm^2; section thickness, 1.4 mm).

Multisection ^{1}H MR spectroscopy acquisition was used to measure the metabolite distribution in the frontal and parietal lobes (Fig 1A), whereas a single-section ^{1}H MR spectroscopy sequence with point-resolved spectroscopy (PRESS) volume

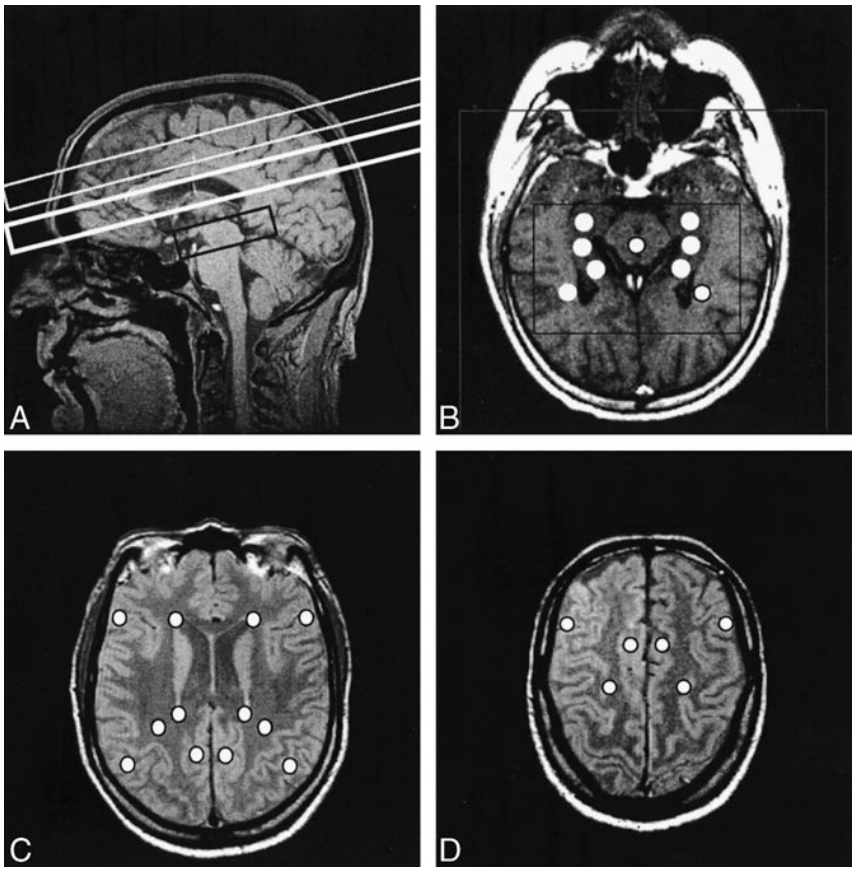

FIG 1. Various MR images are shown for comparison.

A, Sagittal MR image shows outlines of multisection (*two upper boxes*) and PRESS (*lower box*) volumes of interest.

B, Axial T1-weighted MR image shows defined PRESS volume (*inner box*), field of view (*outer box*), and positions of the individual voxels extracted for data analysis (*circles*).

C, Ventricular proton density–weighted axial MR image displaying positions of selected voxels for multisection data analysis (*circles*).

D, Supraventricular proton density–weighted axial MR images displaying positions of selected voxels for multisection data analysis (*circles*).

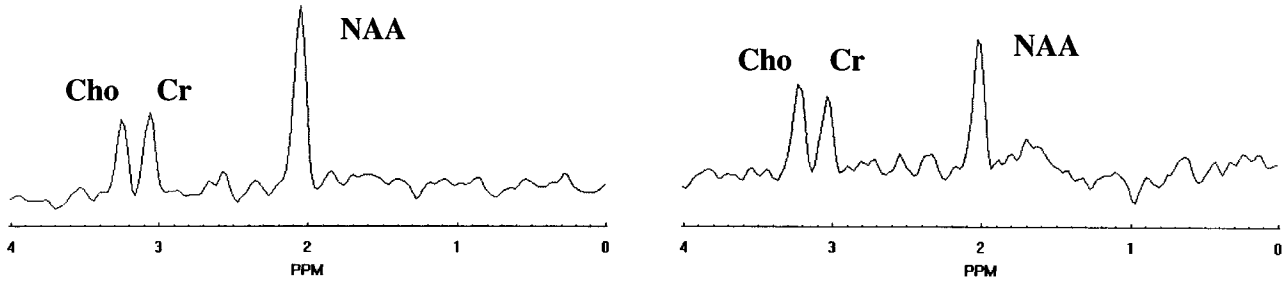

FIG 2. Spectrum selected in normal-appearing white matter (*left*) and spectrum from a white matter signal hyperintensity (*right*) show evident reduction in the NAA peak amplitude at 2.02 ppm in the latter.

preselection (typical size, 70 × 90 × 15 mm^3) was applied covering both hippocampi (Fig 1A). The multisection ^1H MR spectroscopy sequence consisted of two 15-mm-thick sections aligned parallel to the T2-weighted images, with the lower section immediately below the superior extent of the corpus callosum and the other slightly above it (Fig 1A). Lipid contamination of the metabolite spectra was reduced by using a section-selective inversion pulse (inversion time, 170 ms) and was reduced further with the application of k-space extrapolation during data postprocessing (36) (Fig 2). The equivalent of 36 × 36 phase-encoding steps over a circular k-space region was sampled (37), yielding a nominal voxel size of approximately 8 × 8 × 15 mm^3. The data were acquired at 1800/135, resulting in a measurement time of 35 minutes. The PRESS MR spectroscopy sequence used 24 × 24 phase-encoding steps over a circular k-space region with an approximate nominal voxel size of 8.75 × 8.75 × 15 mm^3. The data were acquired with 1800/135, with a measurement time of 13 minutes. Chemical-shift selective saturation water suppression (38) was applied in both MR spectroscopy sequences. The use of a long echo time (135 ms) for the MR spectroscopic studies was decided to reduce lipid contamination. On the other hand, we were unable to detect short T2 metabolites such as *myo*-inositol, which has been implicated in Alzheimer's disease (29), and evaluate NAA, creatine (Cr), and choline changes.

MR Imaging Segmentation and Coregistration with MR Spectroscopy

Segmentation of the MR imaging data was performed using a semiautomated segmentation program developed in-house (39). This software used both T1-weighted and double spin-echo MR image sets (proton density– and T2-weighted images) to assign each MR imaging pixel to a category of gray matter–, white matter–, or CSF-based on the signal-intensity profile. Subsequent interactive manual editing was performed by two trained operators (D.L.A., J.L.T.) to distinguish between sulcal and ventricular CSF and cortical versus subcortical gray matter and to delineate white matter signal hyperintensity and lacunes. Tissue

TABLE 2: Whole brain segmentation

Tissue Type	HC (n = 20)	D + Lac (n = 11)	D (n = 18)	CI + Lac (n = 14)
Ventricular CSF	2.52 ± 1.0	6.14 ± 1.6*	5.51 ± 2.3†	4 ± 1.8
Sulcal CSF	18.74 ± 2.9	23.77 ± 4.2	23.18 ± 2.8†	21.8 ± 3.2
White matter	35.22 ± 2.7	30.30 ± 4.2‡	32.51 ± 3.7‡	33.38 ± 3.0
Cortical GM	42.00 ± 2.4	35.53 ± 2.8*	37.07 ± 2.9†	38.26 ± 3.3
Subcortical GM	1.28 ± 0.3	0.86 ± 0.6	0.96 ± 0.3‡	1.29 ± 0.4
WMSH	0.25 ± 0.4	3.40 ± 2.7†	0.77 ± 0.6§	1.25 ± 1.1

Note.—All data are given as mean ± SD of percentage of total intracranial volume. *P* values from multiple linear regression analysis with adjustment for age and sex. GM, gray matter; WMSH, white matter signal hyperintensity.

*$P < .01$ between patients and HC.

†$P < .001$ between patients and HC.

‡$P < .05$ between patients and HC.

§$P < .01$ between D + Lac and D (with adjustment for MMSE score).

type volumes are expressed as percentages of total intracranial volume.

The segmented MR imaging data were then coregistered with the MR spectroscopy data and converted to the spatial resolution of MR spectroscopy (26). Thus, metabolic signal intensities were coanalyzed with structural data from the same voxel. The tissue composition of each spectroscopy voxel was estimated, taking into account the point-spread function, chemical-shift offset in the MR spectroscopy section direction (for each metabolite), and section profile. This information was used to compute atrophy-corrected metabolic intensities and to test whether metabolic changes were independent of variations of the MR spectroscopy voxel composition.

^{1}H MR Spectroscopy Data Postprocessing

Spectral data processing included zero filling to 1024 data points and 4-Hz gaussian apodization in the time domain and Fourier transformation. The spectra were further phase- and baseline-corrected and curve-fitted using NMR1 software (Tripos Inc., St. Louis, MO). The areas under the peaks of the NAA, Cr, and choline resonances were calculated. To account for instrumental variability among studies, the metabolic signal intensities were referenced to each participant's mean CSF intensity in a region of the lateral ventricles as measured in the proton density–weighted MR images. Finally, the metabolic intensities were atrophy-corrected according to $Met^{corr} = Met/(gm + wm + wmsh)$, where Met^{corr} is the atrophy-corrected metabolic signal intensity, *Met* is the uncorrected signal intensity, and *gm*, *wm*, and *wmsh* are the respective pixel counts of gray matter, white matter, and white matter signal hyperintensity in the voxel as estimated from the coregistered-segmented MR images. The metabolic signal intensities are expressed in an arbitrary scale (institutional units). PRESS and multisection values are not comparable with each other because of the differences in sequence design and voxel size. In addition to the intensity values, metabolic changes are also expressed as NAA/Cr intensity ratios.

Figure 1 (B–D) displays the regions for voxel selection. This was performed using software developed in-house that allows anatomic delineation of regions on coregistered MR images (40). Twenty-seven anatomically predefined regions of interest were selected by a radiologist blinded to the clinical diagnosis (A.A.C.). These regions included the hippocampus, midbrain, and temporal white matter for the PRESS data (Fig 1B), and frontal and parietal cortical and white matter regions for multisection data (Fig 1C and D). Inclusion of white matter signal hyperintensity regions within selected voxels was avoided, but contamination owing to chemical-shift offset and the smaller spatial resolution of MR spectroscopy cannot be ruled out without consulting coregistered segmented images.

Statistical Analysis

Multiple linear regression analysis was performed to test the effect of diagnosis on the spectroscopy and segmentation measures. The regression formula was adjusted for age and sex in all cases and also for MMSE score when patient groups were compared with each other. The reported *P* values are two-tailed. The alpha level was set at 0.05.

To test whether differences in metabolite concentrations across groups were from differences in voxel tissue composition, a two-step analysis was conducted as follows. First a two-tailed Student's *t* test was conducted to determine whether there were significant tissue composition differences in terms of gray/white matter or white matter signal hyperintensity in the same voxels where spectroscopic differences had been found. Second, if such differences turned out to be significant, an analysis of covariance test was performed, with gray matter or white matter signal hyperintensity voxel content as covariants, to determine whether tissue composition made a significant contribution to the metabolic changes. Correlation analysis was performed with the Pearson moment correlation for MR variables and with the Kendall test for MMSE scores.

Results

MR Imaging Segmentation

Table 2 summarizes the results of brain segmentation. Ventricular CSF was 2.52 ± 1.02% in HC volunteers. It was significantly increased in D + Lac patients to 6.14 ± 1.61% ($P = .003$) and in D patients to 5.51 ± 2.27% ($P < .0001$). Sulcal CSF was significantly increased in D patients as compared with HC volunteers ($P = .0001$), whereas in D + Lac patients, there was a trend ($P = .07$) with the regression model used. Cortical gray matter volume in HC volunteers was 42 ± 2.42% and decreased to 35.53 ± 2.81% in D + Lac patients ($P = .002$) and to 37.07 ± 2.89% in D patients ($P < .0001$). White matter volume was also significantly reduced in both demented groups. White matter signal hyperintensity volume was significantly increased in D + Lac patients ($P < .0001$) compared with HC volunteers but not in CI + Lac or D patients. Significant segmentation changes were not observed in CI + Lac patients. When D + Lac and D patient data were compared with each other, white matter signal hyperintensity content was the only segmentation measure that showed a signifi-

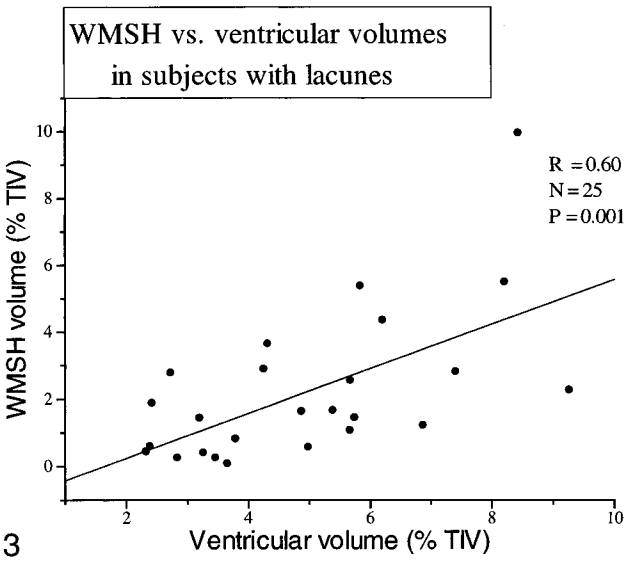

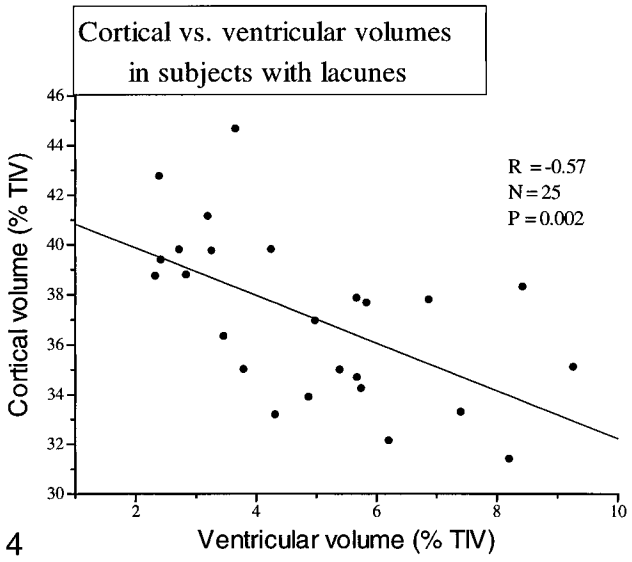

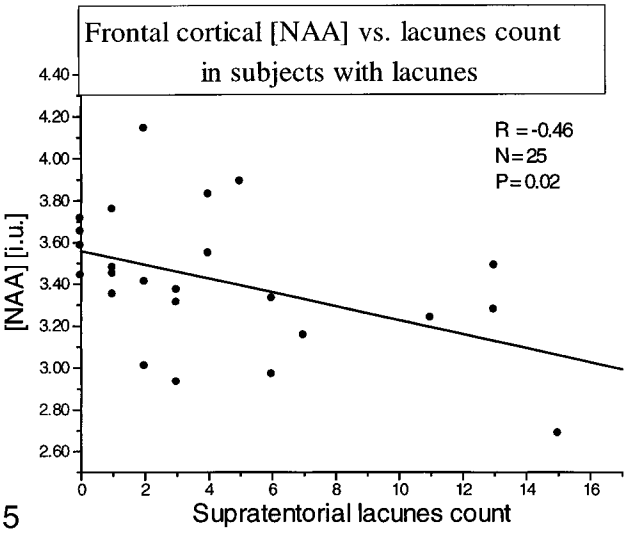

FIG 3. Scatter plot displays the correlation between white matter signal hyperintensity and ventricular volumes for patients with lacunes.

FIG 4. Scatter plot displays the correlation between cortical and ventricular volumes for patients with lacunes.

FIG 5. Scatter plot displays the correlation between frontal cortical NAA and supratentorial lacune count for all patients with lacunes.

cant difference, with the D + Lac patients having 77.3% more white matter signal hyperintensity ($P = .008$).

We also explored the correlation between segmentation measures. Figure 3 shows the correlation between ventricular size and white matter signal hyperintensity volume ($P = .001$) in the patients with lacunes (D + Lac plus CI + Lac). This correlation was also significant, although less strong, in D patients ($P = .024$). Cortical gray matter volume inversely correlated with ventricular CSF among patients with lacunes ($P = .002$) (Fig 4) and in D patients ($P = .014$). No significant correlation was found between ventricular size and either white matter or subcortical gray matter volumes.

^1H Spectroscopy

Table 3 displays regional NAA/Cr ratios for each group. Table 4 shows the corresponding NAA, Cr, and choline values in institutional units. Cortical NAA/Cr (frontal and parietal cortex NAA averaged) in HC volunteers was 2.06 ± 0.22, and NAA was 3.75 ± 0.66. A major finding of this study is that in D + Lac patients, cortical NAA/Cr was reduced to 1.82 ± 0.15 (−11.74%, $P = .007$) and cortical NAA was reduced to 3.37 ± 0.34 (−10.25%, $P = .03$). Significant changes of NAA/Cr or NAA in cortical regions were not observed in D patients. In HC volunteers, white matter NAA/Cr was 2.35 ± 0.31 and NAA was 3.52 ± 0.60. These values were significantly decreased in D + Lac patients to 2.10 ± 0.25 (−10.56%, $P = .01$) and 3.07 ± 0.55 (−12.64%, $P = .04$), respectively. There were no significant changes in white matter in D patients compared with HC volunteers. In HC volunteers, hippocampal NAA/Cr was 1.52 ± 0.14 and NAA was 10.60 ± 0.70. NAA/Cr was significantly reduced in D patients to 1.36 ± 0.16 (−10.33%, $P = .02$). The D + Lac group had no significant changes in the hippocampus compared with the HC group. When D and D + Lac patient data were compared with each other, D patients had lower hippocampal NAA/Cr ($P = .01$). On the oth-

TABLE 3: NAA/Cr ratio

Region	HC (n = 22)	D + Lac (n = 11)	D (n = 19)	CI + Lac (n = 14)
White matter	2.35 ± 0.3	2.10 ± 0.2*	2.35 ± 0.2†	2.28 ± 0.3
Frontal cortex	2.09 ± 0.3	1.80 ± 0.2‡	1.95 ± 0.2§	2.02 ± 0.2‖
Parietal cortex	2.04 ± 0.2	1.85 ± 0.2*	2.03 ± 0.2§	2.00 ± 0.2
Hippocampus	1.52 ± 0.1	1.54 ± 0.3	1.36 ± 0.2*§	1.43 ± 0.2

Note.—*P* values from multiple linear regression with adjustment for age and sex.
*$P < .05$ between patients and HC.
†$P < .01$ between D + Lac and D–with adjustment for MMSE score.
‡$P < .01$ between patients and HC.
§$P < .05$ between D + Lac and D–with adjustment for MMSE score.
‖$P < .05$ betwwen D + Lac and CI + Lac–with adjustment for MMSE score.

er hand, D + Lac patients had lower white matter NAA/Cr ($P = .008$) and NAA ($P = .004$) and also lower cortical NAA/Cr ($P = .03$) and NAA ($P = .03$) than did D patients. D + Lac patients had reduced frontal cortical NAA/Cr compared with CI + Lac patients ($P = .04$). The rest of the spectroscopic changes in the CI + Lac group were not significant. No significant differences were found for Cr and choline when comparing patient groups with the control group. This implies that changes of ratios are primarily from NAA differences and not from variations of Cr or choline.

Results of the ^{1}H MR spectroscopy voxel–tissue composition analysis performed using the coregistered segmented MR images were as follows. No significant differences in white matter signal hyperintensity content in cortical voxels selected for ^{1}H MR spectroscopy analysis were detected between the D + Lac and HC groups. D + Lac patients had less gray matter compared with HC volunteers in cortical ^{1}H MR spectroscopy-selected voxels ($P = .018$ for overall cortex, and $P = .049$ for frontal cortex). Analysis of covariance proved cortical NAA differences to be independent of gray matter content differences. This suggests that the observed metabolite differences in cortical voxels were not simply an artifact of tissue content differences. On the other hand, in the white matter ^{1}H MR spectroscopy-selected voxels, D + Lac patients had significantly more white matter signal hyperintensity volume compared with control volunteers ($P = .001$). Analysis of covariance showed that white matter NAA differences between the D + Lac and control groups were not independent of white matter signal hyperintensity differences ($P = .02$).

Correlation between MR Imaging and ^{1}H MR Spectroscopy Data

Considering all patients with lacunes together (CI + Lac plus D + Lac), frontal cortex NAA was inversely correlated with the number of lacunes ($r = -0.46$, $P = .02$) (Fig 5). Furthermore, frontal cortex NAA inversely correlated with white matter signal hyperintensity volume in all patients with lacunes and in all control volunteers ($r = -0.33$, $P = .02$). A similar correlation was found between white matter NAA and white matter signal hyperintensity volume ($r = -0.35$, $P = .01$). When D + Lac and CI + Lac patients were analyzed separately, CI + Lac had a significant correlation between extent of white matter signal hyperintensity and either frontal cortical NAA ($r = -0.74$, $P = .004$) or white matter NAA ($r = -0.64$, $P = .01$). No significant correlations were found for the D + Lac or D groups. There were no significant correlations between MMSE scores and either structural or metabolic changes for any of the groups.

Discussion

The present study showed cortical metabolic abnormalities in subcortical ischemic vascular dementia. The clinical importance of metabolic changes in vascular dementia was stressed by Mielke et al (18), who found that the severity of dementia was related more to the extent of cortical hypometabolism than to the amount of tissue destruction. ^{1}H MR spectroscopy noninvasively provides biochemical information, which is correlated to metabolic activity (41) and can thus complement structural MR imaging data. Furthermore, cases of Alzheimer's disease and vascular dementia showed different metabolic profiles as revealed by ^{1}H MR spectroscopy, so that differential diagnosis between these two highly prevalent conditions could be improved.

The major findings of this study were as follows. Decreased NAA was found in the cerebral cortex in D + Lac patients independent of atrophy and tissue composition. Furthermore, frontal cortex NAA was inversely correlated with the number of lacunes and volume of white matter signal hyperintensity in all patients with lacunes. Decreased NAA was found in the white matter in D + Lac patients. These NAA changes, however, were not independent of white matter signal hyperintensity voxel content. Decreased hippocampal NAA/Cr was found in D patients but not in D + Lac patients. Increased CSF and decreased cortical gray matter and white matter volumes were found in D patients and D + Lac patients, and increased white matter signal hyperintensity was found in D + Lac

TABLE 4: Atrophy corrected [NAA], [Cr] and choline [Cho]

Region/ metabolite	HC (n = 20)	D + Lac (n = 11)	D (n = 18)	CI + Lac (n = 14)
White matter				
NAA	3.52 ± 0.6	3.07 ± 0.5*	3.64 ± 0.5†	3.22 ± 0.5
Cr	1.54 ± 0.3	1.57 ± 0.3	1.66 ± 0.2	1.48 ± 0.2
Cho	1.48 ± 0.2	1.41 ± 0.26	1.53 ± 0.2	1.43 ± 0.2
Frontal cortex				
NAA	3.72 ± 0.6	3.35 ± 0.31*	3.76 ± 0.4‡	3.45 ± 0.3
Cr	1.84 ± 0.3	1.92 ± 0.2	1.98 ± 0.2	1.76 ± 0.3
Cho	1.51 ± 0.2	1.59 ± 0.3	1.51 ± 0.3	1.49 ± 0.3
Parietal cortex				
NAA	3.80 ± 0.8	3.40 ± 0.5*	3.96 ± 0.6‡	3.57 ± 0.4
Cr	1.90 ± 0.3	1.93 ± 0.4	2.02 ± 0.3	1.84 ± 0.2
Cho	1.39 ± 0.3	1.46 ± 0.4	1.55 ± 0.3	1.41 ± 0.3
Hippocampus				
NAA	10.60 ± 0.7	10.37 ± 1.8	9.89 ± 0.9	10.0 ± 0.8
Cr	7.16 ± 0.7	7.09 ± 1.0	7.47 ± 1.1	7.33 ± 0.8
Cho	7.13 ± 1.0	7.30 ± 0.9	6.72 ± 1.0	7.04 ± 0.6

Note.—All data are presented as institutional units. Data from multislice and PRESS sequences are not comparable owing to technical differences. *P* values derived from multiple linear regression with adjustment for age and sex.

*$P < .05$ between patients and HC.

†$P < .01$ between D + Lac and D–with adjustment for MMSE score.

‡$P < .05$ between D + Lac and D–with adjustment for MMSE score.

patients. There was no significant correlation between MMSE scores and MR imaging volumes or ^{1}H MR spectroscopy values. Taken together, the results show decreased NAA in the cerebral cortex and white matter but not in the hippocampus of patients with subcortical ischemic vascular dementia, suggesting neuronal loss or metabolic impairment in these regions. D patients showed decreased NAA/Cr in the hippocampus. These findings provide further evidence for cortical involvement in dementia associated with subcortical vascular disease.

The first major finding was decreased cortical NAA in D + Lac patients independent of tissue atrophy and composition. Therefore, NAA reduction cannot be explained only by structural changes as detected on MR images. There are several possible explanations for cortical changes occurring with subcortical ischemic vascular dementia. First, the same process of ischemia and infarction that causes lacunes and white matter signal hyperintensity also results in damage to cortical neurons. Partial neuronal loss and laminar necrosis of the cortex have been described in areas remote from the infarction site in cases of hypoxic-hypoperfusion dementia (11). These changes may go undetected on MR images and even by macroscopic pathologic examination (15). An argument against this possibility is that there was no evidence of cortical stroke on the MR images of our D + Lac patients (such patients were excluded from the study).

The second possible explanation for the cortical changes in cases of subcortical ischemic vascular dementia is that primary subcortical injury leads to secondary changes in the cortex. White matter infarction interrupting axons of projection cortical neurons may result in cortical neuronal loss by retrograde degeneration and apoptosis. Additionally, neuronal metabolic impairment results from defferentation (subcortical-cortical diaschisis) secondary to lacunes located particularly in the internal capsule and thalamus (42). To date, there have been few reports on diaschisis with ^{1}H spectroscopy. A clinical case report on crossed cerebellar diaschisis described reduced NAA in the affected cerebellar hemisphere (43). Also, an animal model of transsynaptic injury showed that stretch injury to the optic nerve caused reduced NAA in the lateral geniculate nucleus (44).

The third explanation for cortical changes in the D + L patients is that these patients have concurrent Alzheimer's disease (mixed dementia). It is accepted that the hippocampus is an early and major site for Alzheimer's pathologic abnormalities (21, 45). Hippocampal atrophy detected by MR imaging is characteristic of Alzheimer's disease (46). Our finding that D patients in this study had reduced hippocampal NAA/Cr whereas D + Lac patients did not suggests that the D + Lac patients may not have had Alzheimer's disease. Thus, we tentatively conclude that ischemia or infarction or both in a cortical or subcortical location (with secondary changes in the cortex) caused cortical NAA reductions in the D + Lac patients. Postmortem pathologic study of brains will be required to eliminate the possibility of Alzheimer's disease in these patients definitively.

The significant correlation between frontal cortical NAA with number of lacunes and white matter

signal hyperintensity volume supports the relevance of subcortical damage to frontal cortical impairment. Patients with lacunar dementia present with clinical and neuropsychological evidence of frontal lobe dysfunction (16, 47). This may reflect disruption of frontal subcortical circuits (48) by lacunes located in the thalami and basal ganglia. Pathologic evidence also supports the frontal lobe predilection of lacunes (49). Positron emission tomographic studies (14, 50) of patients with subcortical infarctions depicted reduced cerebral blood flow and metabolic rate more pronounced in the frontal lobes and also found that the severity of dementia was more related to the extent of cortical hypometabolism than to the amount of tissue destruction (18). Finally, previous studies showed that location of subcortical lesions determined the pattern of cortical metabolic abnormalities (14, 42, 51). We, however, did not find an association between lacune location and degree of frontal NAA reduction.

The second major finding was decreased NAA in the white matter of the D + Lac patients as compared with HC volunteers and D patients. This replicates previous findings (25, 26, 31) and is consistent with the deep white matter greater vulnerability to ischemia as it is supplied by long, penetrating, terminal arterioles. The NAA reduction, however, was not independent from white matter signal hyperintensity voxel content. This may indicate that the reduced NAA in white matter is simply a reflection of the extent of white matter signal hyperintensity load. This finding underlines the importance of considering voxel tissue composition when analyzing MR spectroscopy data.

The third major finding was reduced NAA/Cr in the hippocampus of D patients compared with HC volunteers. In contrast, significant hippocampal NAA reduction was not shown in D + Lac patients. The D patients entered in this study had the clinical diagnosis of either probable or possible Alzheimer's disease (Table 1). Reduced NAA in the hippocampal region replicates previous findings (27) and is consistent with neuropathologic studies that showed extensive neuronal loss in the hippocampus in Alzheimer's disease (21, 45). Furthermore, when compared with D + Lac patients, D patients had significantly lower NAA/Cr in the hippocampus. This reduction raises the possibility that decreased hippocampal NAA may be specific to Alzheimer's disease and may be a distinguishing feature from dementia with lacunes. Previous studies (23–26, 28–31) have reported diminished NAA and reduced NAA/Cr in neocortical regions of patients with Alzheimer's disease. These findings, however, could not be replicated in the present study. One possible explanation for this discrepancy is that our multisection acquisition protocol used a steep orientation that did not allow for collecting data from the temporal neocortex and also placed a higher priority on the frontal over the parietal lobe. Consequently, the neocortical areas most vulnerable to Alzheimer's neuropathologic abnormalities were undersampled.

The fourth major finding of this study concerned changes in brain segmentation volumes. D + Lac patients had reduced cortical gray matter volume in the same range as did D patients, as reported previously (26). The marked reduction in cortical volume among patients with exclusive subcortical infarcts on MR images conveys further evidence for the role of cortical changes in cases of subcortical ischemic vascular dementia. Ventricular CSF in D + Lac patients correlated positively with white matter signal hyperintensity volume and inversely with the volumes of cortical gray matter. This suggests that ventricular dilation occurs at the expense of both white matter and cortical volume loss. Ventricular volumes in D patients were also significantly increased compared with HC volunteers, and the difference in ventricular volumes between D patients and D + Lac patients was not significant. The same correlations of ventricular size with white matter signal hyperintensity and cortical volumes applied in D patients, although the significance was less strong. The only segmentation measure that was significantly different between the D + Lac and D groups, however, was volume of white matter signal hyperintensity.

Finally, MMSE scores did not correlate with structural or metabolic measures. The reports in the literature on this topic are controversial; some investigators found that the area of white matter signal hyperintensity correlated to neuropsychological measures (52, 53), whereas others did not (54). Patients with lacunar dementia often present with clinical and neuropsychological evidence of frontal lobe dysfunction (11, 16), but we did not specifically evaluate frontal lobe functioning in the study participants. The D + Lac patients, however, had lower frontal cortical NAA/Cr compared with the CI + Lac patients, and this was the only significantly different MR measure between both groups of patients with lacunes. Of particular note is that neither the number of lacunes nor the volume of white matter signal hyperintensity was statistically different between the D + Lac and CI + Lac groups. We may finally postulate that cortical metabolism is the more relevant factor to cognitive status of patients with lacunes.

There are several limitations in the present study. First, the patient classification was based on the presence of lacunar infarction(s) and dementia, but concurrent degenerative and vascular changes (mixed dementia) cannot be ruled out until histopathologic brain examination is performed. Second, we did not attempt to measure metabolite relaxation times T_1 and T_2 because of the prohibitively long duration of the data acquisition and assumed that the relaxation properties are not different between the groups. It is possible, however, that T_1 and T_2 differ with regions or disease or both. To our knowledge, there is no evidence of abnormal T_1 values in Alzheimer's disease. Christiansen et al

(55), using single-voxel MR spectroscopy, reported prolonged T_2 times for NAA in frontal white matter of patients with Alzheimer's disease compared with control volunteers. If T_2 for NAA were also prolonged in the hippocampus and cortical gray matter, use of the current measurements would have resulted in overestimated NAA measures in Alzheimer's disease and, thus, underestimated differences with the control group. Furthermore, hippocampal volumes were not available at the time of this writing. Metabolite data (including hippocampal voxels), however, were atrophy-corrected using coregistered, segmented MR images. Finally, we selected a small number of MR spectroscopy voxels from different brain regions, which usually include varying amounts of gray matter and white matter because of partial volume effects. Others (56–58) have used automated spectral fitting procedures that allow for the analysis of a large number of voxels from different brain regions. With data from many voxels available, the metabolic changes can be regressed against the voxel tissue composition and estimates of metabolic intensities can be obtained for ''pure'' gray matter and white matter. Current work using a program that automatically fits all spectra will overcome this limitation (59).

Conclusion

This ^{1}H MR spectroscopic study showed a reduction in cortical NAA among patients with dementia with lacunes independent of atrophy and tissue composition. We hypothesize that these changes represent neuronal loss or metabolic impairment or both caused by subcortical injury. Nonetheless, concurrent Alzheimer's-like degeneration cannot be definitively excluded. Patients with Alzheimer's disease showed reduced NAA/Cr in the hippocampus, which is consistent with neuropathologic findings of prominent limbic involvement. Further studies with a larger sample size and postmortem follow-up are needed to substantiate these preliminary findings.

Acknowledgments

We thank Sean Steinman and Camilla Johnson for excellent technical assistance. We are grateful to Dr. Morton A. Lieberman, Director of the University of California, San Francisco Memory Clinic, for referring patients with Alzheimer's disease; Dr. James Mastrianni, for evaluating those patients referred from the University of California, San Francisco Memory Clinic; Dr. Owen Wolkowitz, for referring elderly control volunteers; Dr. Kristine Yaffe, for evaluating the Department of Veterans Affairs Medical Center patients; and Pamela Walton, MS, for recruiting and screening the control volunteers.

References

1. Roman GC. **The epidemiology of vascular dementia.** In: Hartmann A, Kuschinsky W, Hoyer S, eds. *Cerebral Ischemia and Dementia.* Berlin: Springer-Verlag, 1991:9–15
2. Yamaguchi T, Ogata J, Yoshida F. **Epidemiology of vascular dementia in Japan: Proceedings of the NINDS-AIREN International Workshop on Vascular Dementia.** National Institutes of Health, Bethesda, MD, April 19–21, 1991.
3. Suzuki K, Kutsuzawa T, Nakajinia K, Hatano S. **Epidemiology of vascular dementia and stroke in Japan.** In: Hartmann A, Kuschinsky W, Hoyer S, eds. *Cerebral Ischemia and Dementia.* Berlin: Springer-Verlag, 1991:16–24
4. Tomlinson BE, Henderson G. **Some quantitative cerebral findings in normal and demented old people.** In: Terry RD, Gershon S, eds. *Neurobiology of Aging.* New York: Raven Press, 1976
5. Konno S, Meyer JS, Terayama Y, Margishvili GM, Mortel KF. **Classification, diagnosis and treatment of vascular dementia.** *Drugs Aging* 1997;11:361–373
6. Roman GC, Tatemichi TK, Erkinjutti T, et al. **Vascular dementia: diagnostic criteria for research studies: report of the NINDS-AIREN International Workshop.** *Neurology* 1993;43:250–260
7. Miller Fischer C. **Lacunes: small, deep cerebral infarcts.** *Neurology* 1965;15:774–784
8. Englund E, Brun A, Alling C. **White matter changes in dementia of Alzheimer's type: biochemical and neuropathological correlates.** *Brain* 1988;111:1425–1439
9. Roman GC. **From UBOs to Binswanger's disease: impact of magnetic resonance imaging on vascular dementia research.** *Stroke* 1996;27:1269–1273
10. Caplan LR. **Binswanger's disease-revisited.** *Neurology* 1995;45: 626–633
11. De Reuck JL. **Evidence for chronic ischemia in the pathogenesis of vascular dementia: from neuroPATH to neuroPET.** *Acta Neurol Belg* 1996;96:228–231
12. Risberg J, Gustafson L. **Regional cerebral blood flow measurements in the clinical evaluation of demented patients.** *Dement Geriatr Cogn Disord* 1997;8:92–97
13. Mielke R, Kessler J, Szelies B, Herholz K, Wienhard K, Heiss W-D. **Vascular dementia: perfusional and metabolic disturbances and effects of therapy.** *J Neural Transm* 1996[suppl];47:183–191
14. Sultzer DL, Mahler ME, Cummings JL, Van Gorp WG, Hinkin CH, Brown C. **Cortical abnormalities associated with subcortical lesions in vascular dementia: clinical and positron emission tomography findings.** *Arch Neurol* 1995;52:773–780
15. De Reuck J, Decoo D, Marchau M, Santens P, Lemahieu I, Strijckmans K. **Positron emission tomography in vascular dementia.** *J Neurol Sci* 1998;154:55–61
16. Starkstein SE, Sabe L, Vazquez S, et al. **Neuropsychological, psychiatric, and cerebral blood flow findings in vascular dementia and Alzheimer's disease.** *Stroke* 1996;27:408–414
17. Mochizuki Y, Oishi M, Takasu T. **Cerebral blood flow in single and multiple lacunar infarctions.** *Stroke* 1997;28:1458–1460
18. Mielke R, Herholz K, Grond M, Kessler J, Heiss W-D. **Severity of vascular dementia is related to volume of metabolically impaired tissue.** *Arch Neurol* 1992;49:909–913
19. Hachinski VC, Potter P, Merskey H. **Leuko-Araiosis.** *Arch Neurol* 1987;44:21–23
20. Grafton ST, Sumi SM, Stimac GK, Alvord EC, Shaw C-M, Nochlin D. **Comparison of postmortem magnetic resonance imaging and neuropathologic findings in the cerebral white matter.** *Arch Neurol* 1991;48:293–298
21. Brun A, Englund E. **Regional pattern of degeneration in Alzheimer's disease: neuronal loss and histopathological grading.** *Histopathology* 1981;5:549–564
22. Birken DL, Oldendorf WH. **N-acetyl-L-aspartic acid: a literature review of a compound prominent in ^{1}H-NMR spectroscopic studies of brain.** *Neurosci Biobehav Rev* 1989;13:23–31
23. Meyerhoff DJ, MacKay S, Constans J-M, et al. **Axonal injury and membrane alterations in Alzheimer's disease suggested by in vivo proton magnetic resonance spectroscopic imaging.** *Ann Neurol* 1994;36:40–47
24. Constans JM, Meyerhoff DJ, Gerson J, et al. **H-1 MR spectroscopic imaging of white matter signal hyperintensities: Alzheimer disease and ischemic vascular dementia.** *Radiology* 1995;197:517–523
25. MacKay S, Meyerhoff DJ, Constans J-M, Norman D, Fein G, Weiner MW. **Regional gray and white matter metabolite differences in subjects with AD, with subcortical ischemic vascular dementia, and elderly controls with ^{1}H magnetic resonance spectroscopic imaging.** *Arch Neurol* 1996;53:167–174
26. MacKay S, Ezekiel F, Di Sclafani V, et al. **Alzheimer disease and subcortical ischemic vascular dementia: evaluation by combining MR imaging segmentation and H-1 MR spectroscopic imaging.** *Radiology* 1996;198:537–545

27. Schuff N, Amend D, Ezekiel F, et al. **Changes of hippocampal N-acetyl aspartate and volume in Alzheimer's disease: a proton MR spectroscopic imaging and MRI study.** *Neurology* 1997;49:1513–1521
28. Schuff N, Amend D, Meyerhoff D. **Alzheimer disease: quantitative H-1 MR spectroscopic imaging of frontoparietal brain.** *Radiology* 1998;207:91–102
29. Miller BL, Moats RA, Shonk T, Ernst T, Woolley S, Ross BD. **Alzheimer disease: depiction of increased cerebral *myo*-inositol with proton MR spectroscopy.** *Radiology* 1993;187:433–437
30. Tedeschi G, Bertolino A, Lundbom N, et al. **Cortical and subcortical chemical pathology in Alzheimer's disease as assessed by multislice proton magnetic resonance spectroscopic imaging.** *Neurology* 1996;47:696–704
31. Kattapong VJ, Brooks WM, Wesley MH, Kodituwakku PW, Rosenberg GA. **Proton magnetic resonance spectroscopy of vascular- and Alzheimer-type dementia.** *Arch Neurol* 1996;53:678–680
32. Brooks WM, Wesley MH, Kodituwakku PW, Garry PJ, Rosenberg GA. **^{1}H-MRS differentiates white matter hyperintensities in subcortical arteriosclerotic encephalopathy from those in normal elderly.** *Stroke* 1997;28:1940–1943
33. Chui HC, Victoroff JI, Margolin D, Jagust W, Shankle R, Katzman R. **Criteria for the diagnosis of ischemic vascular dementia proposed by the State of California Alzheimer's disease diagnostic and treatment centers.** *Neurology* 1992;42:473–480
34. Jobst KA, Barnetson LPD, Shepstone BJ. **Accurate prediction of histologically confirmed Alzheimer's disease and the differential diagnosis of dementia: the use of NINCDS-ADRDA and DSM-III-R criteria, SPECT, X-ray CT, and Apo E4 in medial temporal lobe dementias.** *Int Psychogeriatr* 1997;9[suppl 1]:: 191–222
35. McKann G, Drachman D, Folstein M, Katzman R, Price D, Stadlan EM. **Clinical diagnosis of Alzheimer's disease: report of the NINCDS-ADRDA Work Group under the auspices of Department of Health and Human Services Task Force on Alzheimer's Disease.** *Neurology* 1984;34:939–944
36. Haupt CI, Schuff N, Weiner MW, Maudsley AA. **Lipid removal in 1H spectroscopic imaging by data extrapolation.** *Magn Reson Med* 1996;35:678–687
37. Maudsley AA, Matson GB, Hugg JW, Weiner MW. **Reduced phase encoding in spectroscopic imaging.** *Magn Reson Med* 1994;31:645–651
38. Haase A, Frahm J, Hänicke W, Matthaei D. **^{1}H NMR chemical shift selective (CHESS) imaging.** *Phys Med Biol* 1985;30:341–344
39. Tanabe J, Amend D, Schuff N, et al. **Tissue segmentation of the brain in Alzheimer's disease.** *Am J Neuroradiol* 1997;18:115–123
40. Maudsley AA, Lin E, Weiner MW. **Spectroscopic imaging display and analysis.** *Magn Reson Imaging* 1992;10:471–485
41. Lu D, Margouleff C, Rubin E. **Temporal lobe epilepsy: correlation of proton magnetic resonance spectroscopy and 18F-fluorodeoxyglucose positron emission tomography.** *Magn Reson Med* 1997;37:18–23
42. Pappata S, Mazoyer B, Tran Dinh S, Cambon H, Levasseur M, Baron JC. **Effects of capsular or thalamic stroke on metabolism in the cortex and cerebellum: a positron tomography study.** *Stroke* 1990;21:519–524
43. Fulham MJ, Dietz MJ, Duyn JH, Shih HH-L, Alger JR, Di Chiro G. **Transsynaptic reduction in N-acetyl-aspartate in cerebellar diaschisis: a proton MR spectroscopic imaging study.** *J Comput Assist Tomogr* 1994;18:697–704
44. Rango M, Spagnoli D, Tomei G, Bamonti F, Scarlato G, Zetta L. **Central nervous system trans-synaptic effects of acute axonal injury: a 1H magnetic resonance spectroscopy study.** *Magn Reson Med* 1995;33:595–600
45. Braak H, Braak E. **Neuropathological stageing of Alzheimer-related changes.** *Acta Neuropathol (Berl)* 1991;82:239–259
46. Jack CR, Petersen RC, O'Brien PC, Tangalos EG. **MR-based hippocampal volumetry in the diagnosis of Alzheimer's disease.** *Neurology* 1992;42:183–188
47. Cummings JL. **Vascular subcortical dementias: clinical aspects.** *Dementia* 1994;5:177–180
48. Cummings JL. **Frontal-subcortical circuits and human behavior.** *Arch Neurol* 1993;50:873–880
49. Ishii N, Nishihara Y, Imamura T. **Why do frontal lobe symptoms predominate in vascular dementia with lacunes?** *Neurology* 1986;36:340–345
50. Mori E, Ishii K, Hashimoto M, Imamura T, Hirono N, Kitagaki H. **The role of functional brain imaging in evaluation of vascular dementia.** Presented at the 3rd International Conference on Harmonization of Dementia Drug Guideline, 1998
51. Chabriat H, Pappata S, Levasseur M, Fiorelli M, Tran Dinh S, Baron JC. **Cortical metabolism in posterolateral thalamic stroke: PET study.** *Acta Neurol Scand* 1992;86:285–290
52. Bondareff W, Raval J, Woo B, Hauser DL, Colletti PM. **Magnetic resonance imaging and the severity of dementia in older adults.** *Arch Gen Psychiatry* 1990;47:47–51
53. Liu CK, Miller BL, Cummings JL, et al. **A quantitative MRI study of vascular dementia.** *Neurology* 1992;42:138–143
54. Giubilei F, Bastianello S, Paolillo A, et al. **Quantitative magnetic resonance analysis in vascular dementia.** *J Neurol* 1997;244: 246–251
55. Christiansen P, Schlosser A, Henriksen O. **Reduced N-acetylaspartate content in the frontal part of the brain in patients with probable Alzheimer's disease.** *Magn Reson Imaging* 1995;13: 457–462
56. Lim KO, Spielman DM. **Estimating NAA in cortical gray matter with applications for measuring changes due to aging.** *Magn Reson Med* 1997;37:372–377
57. Hetherington HP, Pan JW, Mason GF, et al. **Quantitative ^{1}H spectroscopic imaging of human brain at 4.1T using image segmentation.** *Magn Reson Med* 1996;36:21–29
58. Doyle TJ, Bedell BJ, Narayana PA. **Relative concentrations of proton MR visible neurochemicals in gray and white matter in human brain.** *Magn Reson Med* 1995;33:755–759
59. Soher BJ, Young K, Govindaraju V, Maudsley AA. **Automated spectral analysis III: application to in vivo proton MR spectroscopy and spectroscopic imaging.** *Magn Reson Med* 1998;40: 822–831